Inorganic Chemistry

Article

Microporous Lanthanide Metal-Organic Frameworks Containing Coordinatively Linked Interpenetration: Syntheses, Gas Adsorption Studies, Thermal Stability Analysis, and Photoluminescence Investigation

Shengqian Ma,* Daqiang Yuan, Xi-Sen Wang, and Hong-Cai Zhou*

Department of Chemistry, Texas A&M University, P.O. Box 30012, College Station, Texas 77842, and Chemical Sciences & Engineering Division, Argonne National Laboratory, Argonne, Illinois 60439

Received October 15, 2008

Under solvothermal conditions, the reactions of trigonal-planar ligand, TATB (4,4′,4″-*s*-triazine-2,4,6-triyl-tribenzoate) with Dy(NO$_3$)$_3$, Er(NO$_3$)$_3$, Y(NO$_3$)$_3$, Yb(NO$_3$)$_3$, gave rise to four microporous lanthanide metal-organic frameworks (MOFs), designated as PCN-17 (Dy), PCN-17 (Er), PCN-17 (Y), and PCN-17 (Yb), respectively. The four porous MOFs are isostructural, with their crystal unit parameters shrinking in the order of PCN-17 (Dy), PCN-17 (Y), PCN-17 (Er), and PCN-17 (Yb), which also reflects the lanthanides' contraction trend. All of them adopt the novel square-planar Ln$_4$(μ_4-H$_2$O) cluster as the secondary building unit and contain coordinatively linked doubly interpenetrated (8,3)-connected nets. In addition to exhibiting interesting photoluminescence phenomena, the coordinatively linked interpenetration restricts the pore sizes and affords them selective adsorption of H$_2$ and O$_2$ over N$_2$ and CO, as well as renders them with high thermal stability of 500−550 °C as demonstrated from TGA profiles.

Introduction

Metal-organic frameworks (MOFs)[1] have in the past decade become an active research area and attracted great attention from both academia and industry because of their fascinating topology[2] and tantalizing application potential in fields such as catalysis,[3] magnetism,[4] separation,[5] and gas storage.[6] There exists an escalating interest in the synthesis of MOFs using lanthanides owing to their unique optical and magnetic properties and characteristic coordination prefer-

ences.[7] Compared to first-row transition metals, lanthanides have a larger coordination sphere and more flexible coordination geometry. These characteristics make it difficult to control the final topology of a lanthanide MOF.[8] So far, research for reported lanthanide MOFs has been focused on magnetic and photoluminescent properties;[9] however, the construction of porous lanthanide MOFs and their potential application in gas adsorption have been much less developed.[10]

Recently, we have been interested in the use of a trigonal-planar ligand, TATB (4,4′,4″-*s*-triazine-2,4,6-triyl-triben-

* To whom correspondence should be addressed. E-mail: sma@anl.gov (S.M.), zhou@mail.chem.tamu.edu (H.C.Z.).

(1) (a) Eddaoudi, M.; Moler, D. B.; Li, H.; Chen, B.; Reineke, T. M.; O'Keeffe, M.; Yaghi, O. M. *Acc. Chem. Res.* **2001**, *34*, 319–330. (b) Kitagawa, S.; Kitaura, R.; Noro, S. *Angew. Chem., Int. Ed.* **2004**, *43*, 2334–2375. (c) Férey, G. *Chem. Soc. Rev.* **2008**, *37*, 191–214. (d) Suh, M. P.; Cheon, Y. E.; Lee, E. Y. *Coord. Chem. Rev.* **2008**, *252*, 1007–1026.

(2) (a) Ockwig, N. W.; Delgado-Friedrichs, O.; O'Keeffe, M.; Yaghi, O. M. *Acc. Chem. Res.* **2005**, *38*, 176–182. (b) Sun, D.; Collins, D. J.; Ke, Y.; Zuo, J.-L.; Zhou, H.-C. *Chem.—Eur. J.* **2006**, *12*, 3768–3776. (c) Ke, Y.; Collins, D. J.; Sun, D.; Zhou, H.-C. *Inorg. Chem.* **2006**, *45*, 1897–1899. (d) Ma, S.; Fillinger, J. A.; Ambrogio, M. W.; Zuo, J.-L.; Zhou, H.-C. *Inorg. Chem. Commun.* **2007**, *10*, 220–222.

(3) (a) Seo, J. S.; Whang, D.; Lee, H.; Jun, S. I.; Oh, J.; Jeon, Y. J.; Kim, K. *Nature* **2000**, *404*, 982–986. (b) Hu, A.; Ngo, H. L.; Lin, W *J. Am. Chem. Soc.* **2003**, *125*, 11490–11491. (c) Dybtsev, D. N.; Nuzhdin, A. L.; Chun, H.; Bryliakov, K. P.; Konstantin, P.; Talsi, E. P.; Fedin, V. P.; Kim, K. *Angew. Chem., Int. Ed.* **2006**, *118*, 930–934; *Angew. Chem., Int. Ed.* **2006**, *45*, 916−920. (d) Cho, S.-H.; Ma, B.; Nguyen, S. T.; Hupp, J. T.; Albrecht-Schmitt, T. E. *Chem. Commun.* **2006**, 2563−2565; (e) Hwang, Y. K.; Hong, D.-Y.; Chang, J.-S.; Jhung, S. H.; Seo, Y.-K.; Kim, J.; Vimont, A.; Daturi, M.; Serre, C.; Férey, G. *Angew Chem., Int. Ed.* **2008**, *47*, 4144–4148. (f) Horike, S.; Dincǎ, M.; Tamaki, K.; Long, J. R. *J. Am. Chem. Soc.* **2008**, *130*, 5854–5855.

(4) (a) Halder, G. J.; Kepert, C. J.; Moubaraki, B.; Murray, K. S.; Cashion, J. D. *Science* **2002**, *298*, 1762–1765. (b) Janiak, C. *J. Chem. Soc., Dalton Trans.* **2003**, *2781*, 2804.

zoate), to promote the formation of dinuclear and polynuclear secondary building units (SBUs) in porous MOFs constructed from first-row transition metals.[11] Many interesting SBUs such as dinuclear paddlewheel,[11b,f] trinuclear hourglass,[11a,d,g] trinuclear μ_3-oxo-centered basic-carboxylate,[11e] and tetranuclear μ_4-oxo-centered square-planar cluster[11c] have been observed in porous MOFs which demonstrate high surface areas and significant hydrogen uptake.[11] The extraordinary ability of TATB to promote polynuclear SBUs can mainly be attributed to the planarity of the ligand and its tendency to encourage π-π stacking in MOFs.

In continuation of this theme, we have extended the application of the TATB ligand for the construction of lanthanide MOFs with novel architectures and interesting properties.[12] Under solvothermal conditions, the reactions of the TATB ligand with $Dy(NO_3)_3$, $Er(NO_3)_3$, $Y(NO_3)_3$, and $Yb(NO_3)_3$ afforded four microporous lanthanide MOFs, designated as PCN-17 (Dy), PCN-17 (Er), PCN-17 (Y) and PCN-17 (Yb), respectively (PCN represents Porous Coordination Network). The four MOFs are isostructural, and contain coordinatively linked interpenetration which confines their pore sizes for selective adsorption of H_2 and O_2 over N_2 and CO. In this contribution, we present the syntheses and detailed structure description of the four isomorphous MOFs along with the gas adsorption studies, thermal stability analysis, and photoluminescence investigation.

Experimental Section

Synthesis of PCN-17 (Yb). A mixture of H_3TATB (0.01 g) and $Yb(NO_3)_3$ (0.025 g) in 1.2 mL of DMSO (dimethylsulfoxide) with five drops of H_2O_2 (30%, aq.) was sealed in a Pyrex tube, heated to 145 °C (temperature increase rate, 2 °C/min), allowed to stay for 72 h, and cooled to 35 °C (temperature decrease rate, 0.2 °C/min). The brown crystals obtained were washed with DMSO twice to give pure PCN-17 (Yb) with the following formula: $Yb_4(\mu_4\text{-}H_2O)(C_{24}H_{12}N_3O_6)_{8/3}(SO_4)_2 \cdot 3H_2O \cdot 10C_2H_6SO$. Elemental analysis for PCN-17 (Yb), calculated: C 34.71%, H 3.47%, N 3.85%; found: C 33.87%, H 3.41%, N 3.68%.

Synthesis of PCN-17 (Dy). The procedure is similar to the synthesis of PCN-17 (Yb), but with 0.025 g of $Dy(NO_3)_3$ instead of $Yb(NO_3)_3$ used. The resultant brown crystals were washed with DMSO twice to give the pure compound, PCN-17 (Dy), with the formula of $Dy_4(\mu_4\text{-}H_2O)(C_{24}H_{12}N_3O_6)_{8/3}(SO_4)_2 \cdot 3H_2O \cdot 10C_2H_6SO$. Elemental analysis for PCN-17 (Dy), calculated: C 35.22%, H 3.52%, N 3.91%; found: C 33.40%, H 3.47%, N 3.54%.

Synthesis of PCN-17 (Er). The procedure is similar to the synthesis of PCN-17 (Dy), but with 0.025 g of $Er(NO_3)_3$ instead of $Dy(NO_3)_3$ utilized. The resultant pink crystals were washed with DMSO twice to give the pure compound, PCN-17 (Er), with the following formula: $Er_4(\mu_4\text{-}H_2O)(C_{24}H_{12}N_3O_6)_{8/3}(SO_4)_2 \cdot 3H_2O \cdot 10C_2H_6SO$. Elemental analysis for PCN-17 (Er), calculated: C 34.99%, H 3.49%, N 3.88%; found: C 33.61%, H 3.53%, N 3.52%.

Synthesis of PCN-17 (Y). The procedure is similar to the synthesis of PCN-17 (Er), but with 0.025 g of $Y(NO_3)_3$ instead of $Er(NO_3)_3$ utilized. The resultant yellow brown crystals were washed with DMSO twice to give the pure compound, PCN-17 (Y), with the following formula: $Y_4(\mu_4\text{-}H_2O)(C_{24}H_{12}N_3O_6)_{8/3}(SO_4)_2 \cdot 3H_2O \cdot 10C_2H_6SO$. Elemental analysis for PCN-17 (Y), calculated: C 38.98%, H 3.97%, N 4.33%; found: C 37.56%, H 3.93%, N 4.18%. (All the $Ln(NO_3)_3$ used above (Ln = Dy, Er, Y, Yb) were prepared by dissolving Ln_2O_3 in HNO_3 aqua solutions followed by evaporation to crystallize $Ln(NO_3)_3$ salts).

Single-Crystal X-ray Crystallography. Single crystal X-ray data were collected on a Bruker Smart Apex diffractometer

(5) (a) Dybtsev, D. N.; Chun, H.; Yoon, S. H.; Kim, D.; Kim, K. *J. Am. Chem. Soc.* **2004**, *126*, 32–33. (b) Matsuda, R.; Kitaura, R.; Kitagawa, S.; Kubota, Y.; Belosludov, R. V.; Kobayashi, T. C.; Sakamoto, H.; Chiba, T.; Takata, M.; Kawazoe, Y.; Mita, Y. *Nature* **2005**, *436*, 238–241. (c) Dinca, M.; Long, J. R. *J. Am. Chem. Soc.* **2005**, *127*, 9376–9377. (d) Chen, B.; Liang, C.; Yang, J.; Contreras, D. S.; Clancy, Y. L.; Lobkovsky, E. B.; Yaghi, O. M.; Dai, S. *Angew. Chem., Int. Ed.* **2006**, *45*, 1390–1393. (e) Chen, B.; Ma, S.; Zapata, F.; Fronczek, F. R.; Lobkovsky, E. B.; Zhou, H.-C. *Inorg. Chem.* **2007**, *46*, 1233–1236. (f) Chen, B.; Ma, S.; Hurtado, E. J.; Lobkovsky, E. B.; Zhou, H.-C. *Inorg. Chem.* **2007**, *46*, 8490–8492. (g) Chen, B.; Ma, S.; Hurtado, E. J.; Lobkovsky, E. B.; Liang, C.; Zhu, H.; Dai, S. *Inorg. Chem.* **2007**, *46*, 8705–8709. (h) Barcia, P. S.; Zapata, F.; Silva, J. A. C.; Rodrigues, A. E.; Chen, B. *J. Phys. Chem. B* **2007**, *111*, 6101–6103. (i) Humphrey, S. M.; Chang, J.-S.; Jhung, S. H.; Yoon, J. W.; Wood, P. T. *Angew. Chem., Int. Ed.* **2007**, *46*, 272–275. (j) Ma, S.; Sun, D.; Wang, X.-S.; Zhou, H.-C. *Angew. Chem., Int. Ed.* **2007**, *46*, 2458–2462. (k) Ma, S.; Wang, X.-S.; Collier, C. D.; Manis, E. S.; Zhou, H.-C. *Inorg. Chem.* **2007**, *46*, 8499–8501. (l) Bastin, L.; Barcia, P. S.; Hurtado, E. J. J.; Silva, A. C.; Rodrigues, A. E.; Chen, B. *J. Phys. Chem. C* **2008**, *112*, 1575–1181. (m) Li, K. H.; Olsan, D. H.; Lee, J. Y.; Bi, W. H.; Wu, K.; Yuen, T.; Xu, Q.; Li, J. *Adv. Funct. Mater.* **2008**, *18*, 2205–2214.

(6) (a) Chen, B.; Ockwig, N. W.; Millward, A. R.; Contrereas, D. S.; Yaghi, O. M. *Angew. Chem., Int. Ed.* **2005**, *44*, 4745–4749. (b) Millward, A. R.; Yaghi, O. M. *J. Am. Chem. Soc.* **2005**, *127*, 17998–17999. (c) Rowsell, J. L. C.; Yaghi, O. M. *Angew. Chem., Int. Ed.* **2005**, *44*, 4670–4679. (d) Sun, D.; Ke, Y.; Mattox, T. M.; Betty, A. O.; Zhou, H.-C. *Chem. Commun.* **2005**, *544*, 7–5449. (e) Dincǎ, M.; Dailly, A.; Liu, Y.; Brown, C. M.; Neumann, D. A.; Long, J. R. *J. Am. Chem. Soc.* **2006**, *128*, 16876–16883. (f) Collins, D. J.; Zhou, H.-C. *J. Mater. Chem.* **2007**, *17*, 3154–3160. (g) Wang, X.-S.; Ma, S.; Sun, D.; Parkin, S.; Zhou, H.-C. *J. Am. Chem. Soc.* **2006**, *128*, 16474–16475. (h) Ma, S.; Sun, D.; Simmons, J. M.; Collier, C. D.; Yuan, D.; Zhou, H.-C. *J. Am. Chem. Soc.* **2008**, *130*, 1012–1016. (i) Wang, X.-S.; Ma, S.; Rauch, K.; Simmons, J. M.; Yuan, D.; Wang, X.; Yildirim, T.; Cole, W. C.; López, J. J.; de Meijere, A.; Zhou, H.-C. *Chem. Mater.* **2008**, *20*, 3145–3152. (j) Wang, X.-S.; Ma, S.; Forster, P. M.; Yuan, D.; Eckert, J.; López, J. J.; Murphy, B. J.; Parise, J. B.; Zhou, H.-C. *Angew Chem., Int. Ed.* **2008**, *47*, 7263–7266.

(7) (a) Kido, J.; Okamoto, Y. *Chem. Rev.* **2002**, *102*, 2357–2368. (b) Marques, N.; Sella, A.; Takats, J. *Chem. Rev.* **2002**, *102*, 2137–2160.

(8) (a) Long, D.-L.; Blake, A. J.; Champness, N. R.; Wilson, C.; Schroeder, M. *J. Am. Chem. Soc.* **2001**, *123*, 3401–3402. (b) Ghosh, S. K.; Bharadwaj, P. K. *Inorg. Chem.* **2004**, *43*, 2293–2298.

(9) (a) Zhao, B.; Chen, X.-Y.; Cheng, P.; Liao, D.-Z.; Yan, S.-P.; Jiang, Z.-H. *J. Am. Chem. Soc.* **2004**, *126*, 15394–15395. (b) Guo, X.; Zhu, G.; Sun, F.; Li, Z.; Zhao, X.; Li, X.; Wang, H.; Qiu, S. *Inorg. Chem.* **2006**, *45*, 2581–2587. (c) Guo, X.; Zhu, G.; Li, Z.; Chen, Y.; Li, X.; Qiu, S. *Inorg. Chem.* **2006**, *45*, 4065–4070. (d) de Lill, D. T.; Gunning, N. S.; Cahill, C. L. *Inorg. Chem.* **2005**, *44*, 258–266. (e) Chen, B.; Yang, Y.; Zapata, F.; Lin, G.; Qian, G.; Lobkovsky, E. B. *Adv. Mater.* **2007**, *19*, 1693–1696. (f) Chen, B.; Wang, L.; Zapata, F.; Qian, G.; Lobkovsky, E. B. *J. Am. Chem. Soc.* **2008**, *130*, 6718–6719.

(10) (a) Pan, L.; Adams, K. M.; Hernandez, H. E.; Wang, X.; Zheng, C.; Hattori, Y.; Kaneko, K. *J. Am. Chem. Soc.* **2003**, *125*, 3062–3067. (b) Devic, T.; Serre, C.; Audebrand, N.; Marrot, J.; Férey, G. *J. Am. Chem. Soc.* **2005**, *127*, 12788–12790. (c) Chandler, B. D.; Yu, J. O.; Cramb, D. T.; Shimizu, G. K. H. *Chem. Mater.* **2007**, *19*, 4467–4473.

(11) (a) Sun, D.; Ma, S.; Ke, Y.; Petersen, T. M.; Zhou, H.-C. *Chem. Commun.* **2005**, *2663*, 2665. (b) Sun, D.; Ma, S.; Ke, Y.; Collins, D. J.; Zhou, H.-C. *J. Am. Chem. Soc.* **2006**, *128*, 3896–3897. (c) Ma, S.; Zhou, H.-C. *J. Am. Chem. Soc.* **2006**, *128*, 11734–11735. (d) Sun, D.; Ke, Y.; Collins, D. J.; Lorigan, G. A.; Zhou, H.-C. *Inorg. Chem.* **2007**, *46*, 2725–2734. (e) Ma, S.; Wang, X.-S.; Manis, E. S.; Collier, C. D.; Zhou, H.-C. *Inorg. Chem.* **2007**, *46*, 3432–3434. (f) Ma, S.; Sun, D.; Ambrogio, M. W.; Fillinger, J. A.; Parkin, S.; Zhou, H.-C. *J. Am. Chem. Soc.* **2007**, *129*, 1858–1859. (g) Yu, C.; Ma, S.; Pechan, M. J.; Zhou, H.-C. *J. Appl. Phys.* **2007**, *101*, 09E108. (h) Ma, S.; Eckert, J.; Forster, P.; Yoon, J.; Hwang, Y. K.; Chang, J.-S.; Collier, C. D.; Parise, J. B.; Zhou, H.-C. *J. Am. Chem. Soc.* **2008**, *130*, 15896–15902.

(12) Ma, S.; Wang, X.-S.; Yuan, D.; Zhou, H.-C. *Angew. Chem., Int. Ed.* **2008**, *47*, 4130–4133.

Table 1. Crystal Data[a] and Structure Refinement of PCN-17 (Dy), PCN-17 (Er), PCN-17 (Y), and PCN-17 (Yb)

	PCN-17 (Dy)	PCN-17 (Er)	PCN-17 (Y)	PCN-17 (Yb)
formula	$C_{72}H_{62}N_8O_{31}S_6Dy_4$	$C_{72}H_{62}N_8O_{31}S_6Er_4$	$C_{72}H_{62}N_8O_{31}S_6Y_4$	$C_{72}H_{62}N_8O_{31}S_6Yb_4$
FW	2377.66	2396.70	2083.30	2419.82
crystal system	cubic	cubic	cubic	cubic
space group	$Im\bar{3}m$	$Im\bar{3}m$	$Im\bar{3}m$	$Im\bar{3}m$
a, Å	26.348(3)	26.268(4)	26.311(3)	26.225 (1)
b, Å	26.348(3)	26.268(4)	26.311(3)	26.225(1)
c, Å	26.348(3)	26.268(4)	26.311(3)	26.225(3)
α, deg	90.00	90.00	90.00	90.00
β, deg	90.00	90.00	90.00	90.00
γ, deg	90.00	90.00	90.00	90.00
V, Å^3	18292(3)	18126(5)	18214(4)	18037(2)
Z	6	6	6	6
d_{cacl}, g/cm^3 cm-1	1.295	1.317	1.09	1.337
GOF	1.033	1.079	1.107	1.094
R_1, wR_2[b]	0.0601, 0.1668	0.0947, 0.2529	0.0921, 0.2555	0.0969, 0.2685

[a] Obtained with graphite-monochromated Mo Kα (λ = 0.71073 Å) radiation, [b] $R_1 = \sum||F_o| - |F_c||/\sum|F_o|$ and $wR_2 = \{[\sum w(F_o^2 - F_c^2)^2]/[\sum w(F_o^2)^2]\}^{1/2}$.

equipped with an Oxford Cryostream low temperature device and a fine-focus sealed-tube X-ray source (Mo Kα radiation, λ = 0.71073 Å, graphite monochromated) operating at 45 kV and 35 mA. Frames were collected with 0.3° intervals in φ and ω for 30 s per frame such that a hemisphere of data was collected. Raw data collection and refinement were done using SMART. Data reduction was performed using SAINT+ and corrected for Lorentz and polarization effects.[13] The structure was solved by direct methods and refined by full-matrix least-squares on F^2 with anisotropic displacement using SHELX-97.[14] Non-hydrogen atoms were refined with anisotropic displacement parameters during the final cycles. Hydrogen atoms on carbon were calculated in ideal positions with isotropic displacement parameters set to $1.2 \times U_{eq}$ of the attached atom. Absorption corrections were applied using SADABS after the formula of the compound is determined approximately.[13] Solvent molecules in the structure were highly disordered and were impossible to refine using conventional discrete-atom models. To resolve these issues, the contribution of solvent electron density was removed by the SQUEEZE routine in PLATON.[15] In all of the four structures, the Ln (Ln = Yb, Er, Dy, Y) atoms are disordered and each Ln is refined as occupying two equally populated positions. CCDC-617998 (PCN-17 (Yb)) and CCDC-644651 (PCN-17 (Dy)) contain the supplementary crystallographic data which can be obtained free of charge at www.ccdc.cam.ac.uk/conts/retrieving.html (or from the Cambridge Crystallographic Data Center, 12, Union Road, Cambridge CB21EZ, UK; fax: (+44) 1223−336−033; or deposit@ccdc.cam.ac.uk).

Gas Adsorption Measurements. Gas adsorption measurements were performed with a Beckman Coulter SA 3100 surface area and pore size analyzer. The fresh samples were evacuated under dynamic vacuum (<10^{-3} torr) at 250 °C overnight to remove the guest molecules. Before the measurement, each sample was evacuated again by using the "outgas" function of the surface area analyzer for 2 h at 250 °C. A sample of 100 mg was used for N_2 (99.999%) adsorption measurement, and was maintained at 77 K with liquid nitrogen. In the hydrogen adsorption measurement, high purity hydrogen (99.9995%) was used. The regulator and pipe were flushed with hydrogen before connecting to the analyzer. The internal lines of the instrument were flushed three times by utilizing the "flushing lines" function of the program to ensure the purity of H_2. The measurement was maintained at 77 K with liquid nitrogen. Similar to the procedures used for H_2 measurement at 77 K, highly

pure O_2 (99.99%), CO (99.99%), and CO_2 (99.99%) were used for their respective gas adsorption measurements. All the gases used for the measurements were purchased from Linde Gas LLC, Cincinnati, Ohio, U.S.A. The temperatures at 195 K were maintained with an acetone-dry ice bath. To prevent condensation of CO and O_2 at 77 K, the pressure ranges were below 448 torr and 156 torr, respectively. For all adsorption isotherms, P_0 represents a relative saturation pressure given by the Beckman Coulter SA 3100 surface area and pore size analyzer during the measurements: at 77 K, P_0 was 757 torr for N_2, 441 torr for CO, and 151 torr for O_2. For hydrogen 757 torr was used as a relative standard.

Results and Discussion

Description of the Structures. Single crystal X-ray analysis revealed that the four MOFs are isostructural with each other, crystallizing in space group $Im\bar{3}m$ (Table 1). The trend of lanthanide contraction from Dy to Yb can be reflected by the reduction in their unit cell parameters as shown in Table 1. The unit parameters of PCN-17 (Y) lie in between PCN-17 (Er) and PCN-17 (Dy) and can be ascribed to the Y^{3+} ion radius of 1.02 Å which is between the radius of Er^{3+} (1.00 Å) and that of Dy^{3+} (1.03 Å).[16] The four MOFs all adopt the square-planar $Ln_4(\mu_4\text{-}H_2O)$ SBU (Ln = Dy, Er, Y, Yb), with the $\mu_4\text{-}H_2O$ residing at the center of the square of four Ln atoms (Figure 1a). All of the four Ln atoms in the SBU are in the same plane and coordinate seven oxygen atoms (four from four carboxylate groups of four different TATB ligands, two from the bridging sulfate ligand generated in situ, and one from the $\mu_4\text{-}H_2O$). The distances between the Ln and carboxylate oxygen range from 2.152 Å to 2.187 Å, and those of Ln and sulfate oxygen fall in the range of 2.147 to 2.324. The Ln−μ_4-H_2O distances vary from 2.703 to 3.008 Å, indicating very weak Ln−H_2O bonding (Table 2). The μ_4-H_2O bridged square-planar structural motif has been previously observed in some lanthanide complexes,[17] but it is slightly different from that in PCN-9 where a μ_4-O atom resides at the center of a square of four cobalt atoms.[11c] The rationale for the assignment of the μ_4-center as H_2O molecule instead of O atom lies in the charge balance of the whole framework.

(13) *SAINT+*, version 6.22; Bruker Analytical X-Ray Systems, Inc.: Madison, WI, 2001.

(14) Sheldrick, G. M. *SHELX-97*; Bruker Analytical X-Ray Systems, Inc.: Madison, WI, 1997.

(15) Spek, A. L. *J. Appl. Crystallogr.* **2003**, *36*, 7–13.

(16) Lide, D. R. *Handbook of Chemistry and Physics*, 73rd ed.; CRC Press, Int.: Boca Raton, FL, 1992−1993.

(17) Deacon, G. B.; Forsyth, C. M.; Harika, R.; Junk, P. C.; Ziller, J. W.; Evans, W. J. *J. Mater. Chem.* **2004**, *14*, 3144–3149.
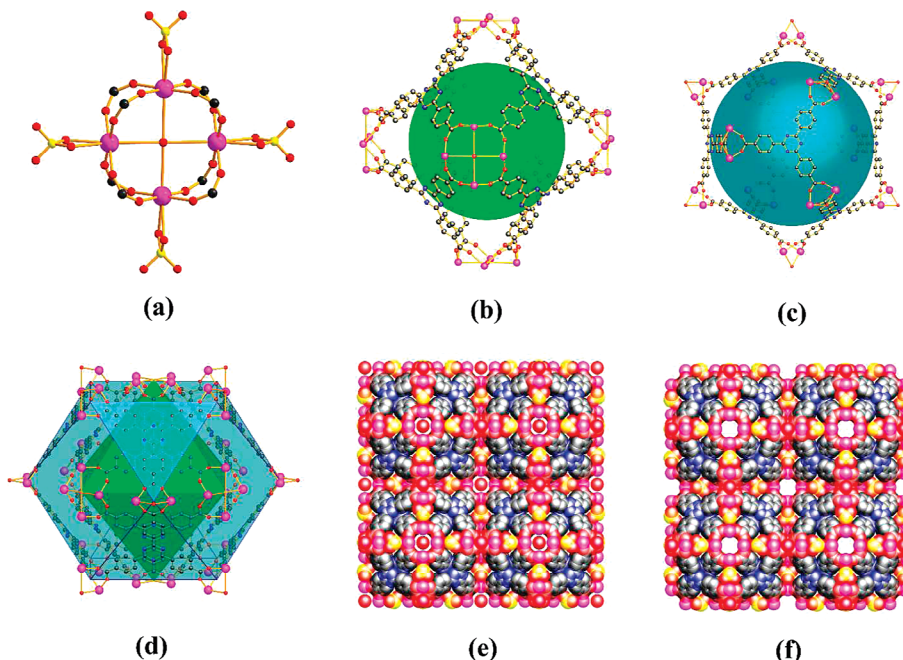
Figure 1. Structures of PCN-17 (Dy, Er, Y, Yb): (a) $Ln_4(\mu_4\text{-}H_2O)$ SBUs; (b) octahedral cage; (c) cuboctahedral cage; (d) an octahedral cage enclosed by an cuboctahedral cage form from another network; (e) space-filling packing of unactivated sulfate-bridging doubly interpenetrated (8,3)-connected net (viewed from (1 0 0) direction); (f) space-filling packing of activated sulfate-bridging doubly interpenetrated (8,3)-connected net with open tiny pores resulted from the removal of the $\mu4\text{-}H_2O$ of the SBUs (viewed from (1 0 0) direction). (Pink, Ln (Ln = Dy, Er, Y, Yb); gray, carbon; red, oxygen; yellow, sulfur).

Table 2. Selective Bond Distances of PCN-17 (Dy), PCN-17 (Er), PCN-17 (Y), and PCN-17 (Yb)

	PCN-17 (Dy)	PCN-17 (Er)	PCN-17 (Y)	PCN-17 (Yb)
Ln-O (carboxylate)/Å distances (Å)	2.187	2.160	2.168	2.152
Ln-O (sulfate)/Å distances (Å)	2.324	2.147	2.268	2.198
Ln-μ_4-H_2O/Å distances (Å)	2.819	2.776	3.008	2.703
Ln-Ln (opposite) distances of $Ln_4(\mu_4$-$H_2O)$ SBUs/Å	6.392	6.407	6.584	6.335
π-π interaction of the TATB ligand pairs/Å	3.351	3.394	3.473	3.441

In all of the four structures, every TATB ligand links three $Ln_4(\mu_4$-$H_2O)$ SBUs, every $Ln_4(\mu_4$-$H_2O)$ SBU connects eight trigonal-planar TATB ligands and four sulfate ligands to form an infinite framework (Supporting Information, Figure S1a). Alternatively, they can be viewed comprising the infinite SBU with each sulfate bridging two $Ln_4(\mu_4$-$H_2O)$ clusters and each cluster connecting four sulfates (Supporting Information, Figure S1b). There exist two types of cages in their structures: one is a truncated octaheral cage defined by six $Ln_4(\mu_4$-$H_2O)$ SBUs at the corners and eight TATB ligands on the faces (Figure 1b), and the other one is a cuboctahedral cage enclosed by eight truncated octahedral cages occupying the vertices of the cube (Figure 1c). Every cuboctahedral cage connects eight truncated octahedral cages via face-sharing, and each truncated octahedral cage links six cuboctahedral cages to form a (8,3)-net framework (Supporting Information, Figure S2).

Two such (8,3)-nets are mutually interpenetrated because of the π-π interactions of the TATB ligand pairs (Supporting Information, Figure S3) as reflected in the short distance between the centers of the two triazine rings of the TATB ligand pairs (Table 2). The staggered TATB ligand pairs resulting from strong π-π interactions lead to the truncated octahedral cages of one set framework enclosed by the cuboctahedral cages of the other set framework with the triangular face-sharing (Figure 1d). This closes the windows of the truncated octahedral cages and also reduces the size

of the opening of the cuboctahedral cages, which is further restricted by the bridging sulfate ligands. Overall, their structures can be described as sulfate-bridged doubly interpenetrated (8,3)-connected nets. When using the space-filling model to pack their frameworks, no open pores can be found along (1 0 0) direction (Figure 1e) or (1 1 0) direction (Supporting Information, Figure S4a), although some tiny open pores (~ 2.0 Å) can be observed along (1 1 1) direction (Supporting Information, Figure S4b). However, the removal of the μ_4-H_2O in the $Ln_4(\mu_4$-$H_2O)$ SBUs can result in some openings of ~3.5 Å which are the only passages to allow gas molecules to pass through (Figure 1f).

Gas Adsorption Studies. To test their permanent porosities, gas adsorption studies were performed utilizing fully activated samples. Unlike our previous reported porous MOFs,[11] soaking freshly prepared PCN-17 (Dy, Er, Y, Yb) in methanol and dichloromethane could not remove the high-boiling-point H_2O and DMSO guest molecules, and the solvent-exchanged samples took up neither N_2 nor H_2 even after thermal activation at 100 °C. This can be attributed to retention of the μ_4-H_2O in the $Ln_4(\mu_4$-$H_2O)$ SBU, which precludes the entrance of methanol or dichloromethane for solvent exchange despite the existence of small openings of ~2.0 Å along (1 1 1) direction (excluding van der Waals radii[18]). Alternatively, the four porous MOFs were then

(18) Bondi, A. *J. Phys. Chem.* **1964**, *68*, 441–451.
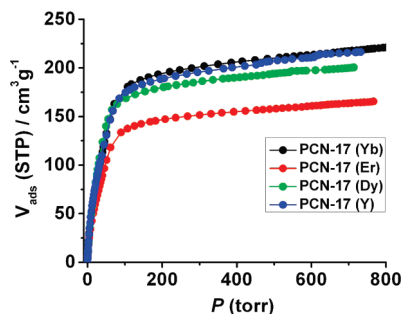
Figure 2. CO_2 adsorption isotherms of PCN-17 (Dy, Er, Y, Yb) at 195 K.

Table 3. Gas Adsorption Summary of PCN-17 (Dy), PCN-17 (Er), PCN-17 (Y), and PCN-17 (Yb)

	PCN-17 (Dy)	PCN-17 (Er)	PCN-17 (Y)	PCN-17
BET surface area $(m^2/g)^a$	738	606	814	820
pore volume $(cm^3/g)^b$	0.31	0.25	0.33	0.34
H_2 uptake (cm³/g, at 77K, 1 atm)	110	90	123	105
selectivity of O_2 over N_2 (at $P/P_0 = 1$)	2.3	2.5	1.9	9.0
selectivity of H_2 over CO (at $P/P_0 = 1$)	1.9	1.5	1.7	3.6

^{a} Calculated with CO_2 adsorption data at 195 K using the Brunauer–Emmett–Teller (BET) equation. ^{b} Calculated with CO_2 adsorption data at 195 K using Dubinin–Radushkevich equation.

activated in a way similar to the activation of PCN-17 (Yb)[12] by evacuating the freshly prepared samples at 250 °C under a dynamic vacuum overnight. Considering their limited pore size of ∼3.5 Å even after the removal of the μ_4-H_2O in the $Ln_4(\mu_4$-$H_2O)$ SBUs, CO_2 (kinetic diameter: 3.33 Å[19]) adsorption isotherms measured at 195 K instead of N_2 (kinetic diameter: 3.64 Å[19]) adsorption isotherms measured at 77 K were employed to estimate their surface areas. As shown in Figure 2, CO_2 adsorption isotherms of the four fully activated MOFs reveals typical type-I behaviors as expected for microporous materials. Fittings of the Brunauer–Emmett–Teller (BET) equation[20] to the adsorption isotherms of CO_2 give the estimated surface areas of 738 m²/g, 606 m²/g, 814 m²/g, and 820 m²/g for PCN-17 (Dy), PCN-17 (Er), PCN-17 (Y), and PCN-17 (Yb), respectively (Table 3). Using the Dubinin–Radushkevich equation,[21] the pore volumes of PCN-17 (Dy), PCN-17 (Er), PCN-17 (Y), and PCN-17 (Yb) are estimated to be 0.31 cm³/g, 0.25 cm³/g, 0.33 cm³/g, and 0.34 cm³/g respectively (Table 3).

To check their potential for selective gas adsorption applications, N_2, H_2, O_2, and CO adsorption studies were carried out at 77 K. As shown in Figure 3, all of the four porous MOFs can adsorb a large amount of O_2 (258 cm³/g for PCN-17 (Dy), 196 cm³/g for PCN-17 (Er), 170 cm³/g for PCN-17 (Y), and 210 cm³/g for PCN-17 (Yb)) and a moderate amount of H_2 (110 cm³/g for PCN-17 (Dy), 90 cm³/g for PCN-17 (Er), 123 cm³/g for PCN-17 (Y), and 105 cm³/g for PCN-17 (Yb)) with typical type-I behaviors. This indicates that O_2 and H_2 molecules can pass through their

(19) Beck, D. W. *Zeolite Molecular Sieves;* Wiley & Sons: New York, 1974.
(20) Brunauer, S.; Emmett, P. H.; Teller, E. *J. Am. Chem. Soc.* **1938**, *60*, 309–319.
(21) Dubinin, M. M.; Radushkevich, L. V. *Dokl. Akad. Nauk USSR* **1947**, *55*, 327–329.
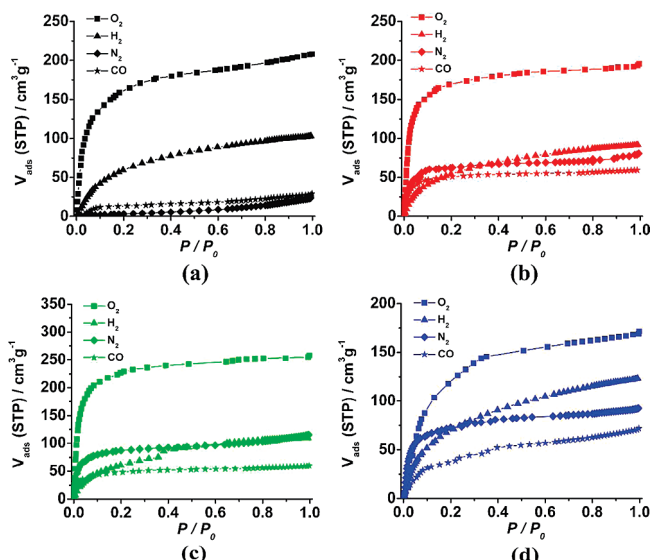
Figure 3. O_2, H_2, N_2, and CO adsorption isotherms of (a) PCN-17 (Yb); (b) PCN-17 (Er); (c) PCN-17 (Dy); (d) PCN-17 (Y) at 77 K.

pores freely (Table 3). However, the amounts of N_2 and CO adsorbed by PCN-17 (Yb) are very limited, and the selectivity of H_2 over CO is 3.6 but the selectivity of O_2 over N_2 is 9.0 (Table 3). Nevertheless, PCN-17 (Dy, Er, Y) can uptake moderate amounts of N_2 and CO with type-I behaviors. The volumes of adsorbed N_2 and CO by PCN-17 (Dy, Er, Y) are comparable or lower than the volumes of adsorbed H_2 despite the fact that H_2 is a supercritical gas at 77 K and are much lower than those of adsorbed O_2. This indicates that the pore sizes of PCN-17 (Dy, Er, Y) are not open enough to let N_2 and CO gas molecules go through freely. The selectivity of H_2 over CO is 1.9, 1.5, and 1.7 for PCN-17 (Dy), PCN-17 (Er), and PCN-17 (Y), respectively, while the selectivity of O_2 over N_2 is 2.3, 2.5, and 1.9 (Table 3). In view of the kinetic diameters of 2.89 Å for H_2, 3.46 Å for O_2, 3.64 Å for N_2, and 3.76 Å for CO,[21] it can be inferred that the pore opening of PCN-17 (Yb) should be between 3.46 and 3.64 Å in diameter, and those of PCN-17 (Er), PCN-17 (Dy), and PCN-17 (Y) should be around 3.7 Å. These are also consistent with the crystallographically observed aperture sizes (Ln-Ln distances in Table 2) of the four MOFs. The different aperture sizes of the four porous MOFs may presumably ascribe for the difference of their sorption properties. The adsorption selectivity of H_2 and O_2 over N_2 and CO shown by PCN-17 is not common,[5a,c,h,j] promising its application in the separation of nitrogen and oxygen, as well as the separation of hydrogen from carbon monoxide in fuel cell applications.

Thermal Stability Analysis. To investigate their thermal stabilities, thermal gravimetric analysis (TGA) was performed on a Perkin-Elmer TGA 7 instrument. As shown in Figure 4, PCN-17 (Dy)/(Er)/(Yb) have similar thermal stability and are stable up to 500 °C. The first weight loss from 20 to 430 °C corresponds to the loss of 10 DMSO, 3 H_2O guest solvent molecules, and 1 μ_4-H_2O molecule, which is followed by a steady plateau up to 500 °C. Their frameworks start to collapse with the loss of TATB ligands from 500 to 700 °C. As for PCN-17 (Y), it is stable up to 550 °C followed by
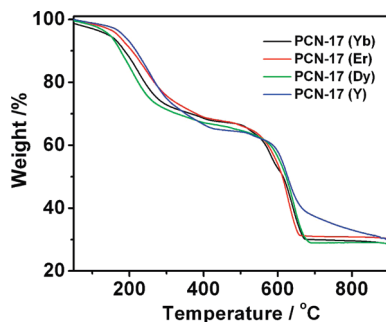
Figure 4. TGA profiles of PCN-17 (Dy, Er, Y, Yb).
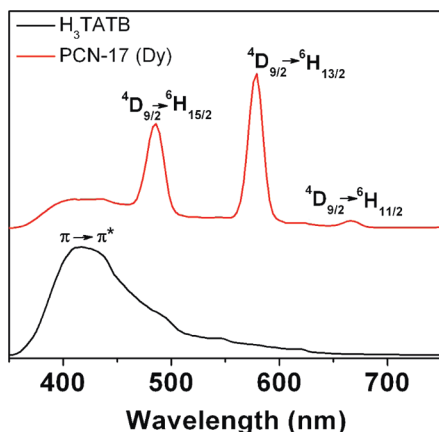
Figure 5. Room temperature solid-state photoluminescence spectra of H$_3$TATB and PCN-17 (Dy).

the decomposition of its framework with the loss of three TATB ligands. Their thermal stabilities demonstrated from TGA profiles are among the highest of reported porous MOFs,[22] albeit some dense structures can be stable up to 600 °C.[23] Their unusual stabilities can be attributed to the coordinatively linked interpenetration. Nevertheless, H$_2$ adsorption isotherms of the samples heated at high temperatures revealed they could only maintain their framework integrities at up to 480 °C (Supporting Information, Figure S5).[12]

Photoluminescent Investigation. Lanthanide compounds are known for their photoluminescent properties.[9] Excited at 325 nm at room temperature, H$_3$TATB exhibits a broad emission band at ∼ 420 nm (Figure 5), which can be ascribed

to the intraligand π to π^* transitions.[11a,d] As shown in Figure 4, PCN-17 (Dy) exhibits characteristic Dy^{3+} emissions resulted from the $^4F_{9/2} \rightarrow {}^6H_J$ (J = 15/2, 13/2, and 11/2) transitions: the emission band at ∼ 485 nm corresponds to the $^4F_{9/2} \rightarrow {}^6H_{15/2}$ transition; the band at ∼579 nm arises from the $^4F_{9/2} \rightarrow {}^6H_{13/2}$ transition; and the weak band at ∼667 nm is attributed to the $^4F_{9/2} \rightarrow {}^6H_{11/2}$ transition.[24] Only very weak intraligand fluorescent emission from the TATB ligand has been observed, and no charge transfer bands have been found because the energy transfer between TATB and Dy^{3+} is inefficient.[11a,d,25]

Conclusions

In summary, four isostructural lanthanide microporous MOFs, PCN-17 (Dy, Er, Y, Yb) based on novel square-planar Ln$_4$(μ_4-H$_2$O) SBUs have been constructed and structurally described. They contain coordinatively linked interpenetration which not only yields high thermal stability up to 550 °C as demonstrated from TGA profiles but also confines their pore sizes affording interesting gas adsorption properties. The selective adsorption of H$_2$ and O$_2$ over N$_2$ and CO exhibited by PCN-17 (Yb) promises its potential applications in the separation of nitrogen and oxygen, the separation of hydrogen from carbon monoxide in fuel cell applications, and hydrogen enrichment of the N$_2$/H$_2$ exhaust in ammonia synthesis.

Supporting Information Available: Further details are given in crystallographic information files (CIF) of PCN-17 (Er, Y), with structure graphics, and in Figures S1−S5. This material is available free of charge via the Internet at http://pubs.acs.org.

IC801948Z

(22) Park, K. S.; Ni, Z.; Côté, A. P.; Choi, J. Y.; Huang, R.; Uribe-Romo, F. J.; Chae, H. K.; O'Keeffe, M.; Yaghi, O. M. *Proc. Nat. Acad. Sci. U.S.A.* **2006**, *103*, 10186–10191.

(23) de Lill, D. T.; Cahill, C. L. *Chem. Commun.* **2006**, *4946*, 4948.

(24) (a) Chandler, B. D.; Cramb, D. T.; Shimizu, G. K. H. *J. Am. Chem. Soc.* **2006**, *128*, 10403–10412. (b) Sun, Y.-Q.; Zhang, J.; Yang, G.-Y. *Chem. Commun.* **2006**, *1947*, 1949. (c) Sun, Y.-Q.; Zhang, J.; Yang, G.-Y. *Chem. Commun.* **2006**, *4700*, 4702.

(25) Thirumurugan, A.; Pati, S. K.; Green, M. A.; Natarajan, S. *J. Mater. Chem.* **2003**, *13*, 2937–2941.